Synergistic Effects in the Activity of Nano-Transition-Metal Clusters Pt 12 M (M = Ir, Ru or Rh) for NO Dissociation

Jelle Vekeman, Qing Wang, Xavier Deraet, Dominique Bazin, Frank de Proft, Hazar Guesmi, Frederik Tielens

Synergistic Effects in the Activity of Nano-Transition-Metal Clusters $Pt_{12}M$ (M = Ir, Ru or Rh) for NO Dissociation

Jelle Vekeman,*[1] Qing Wang,[2] Xavier Deraet,[3] Dominique Bazin,[4,5] Frank De Proft,[3] Hazar Guesmi,[2] and Frederik Tielens*[3]

[1] Center for Molecular Modeling (CMM) Ghent University Technologiepark-Zwijnaarde 46, 9052 Zwijnaarde, Belgium.

[2] ICGM, Université Montpellier, CNRS, EMSCM Montpellier France

[3] Eenheid Algemene Chemie (ALGC) Vrije Universiteit Brussel (VUB) Pleinlaan 2, 1050 Brussel, Belgium

[4] Institut de Chimie Physique, Université Paris-Sud, UMR CNRS 8000, Bâtiment 350, Avenue Jean Perrin 15, 91405 Orsay Cedex, France

[5] Laboratoire de Physique des Solides, Université Paris-Sud, UMR CNRS 8502, Bâtiment 510 Rue Nicolas Appert, 91405 Orsay Cedex, France

E-mails: jelle.vekeman@ugent.be, frederik.tielens@vub.be

Supporting information for this article is given via a link at the end of the document.

Abstract**:** The dissociation of environmentally hazardous NO through dissociative adsorption on metallic clusters supported by oxides, is receiving growing attention. Building on previous research on monometallic M_{13} clusters [*The Journal of Physical Chemistry C* **2019**, *123* (33), 20314–20318], this work considers bimetallic $Pt_{12}M$ (M = Rh, Ru or Ir) clusters. The adsorption energy and activation energy of NO dissociation on the clusters have been calculated in vacuum using Kohn-Sham DFT, while their trends were rationalized using reactivity indices such as molecular electrostatic potential and global Fermi softness. The results show that doping of the Pt clusters lowered the adsorption energy as well as the activation energy for NO dissociation. Furthermore, reactivity indices were calculated as a first estimate of the performance of the clusters in realistic amorphous silica pores (MCM-41) through *ab initio* molecular dynamics simulations.

Introduction

Platinum-, palladium- and rhodium-based catalysts are widely used to remove environmentally toxic nitrogen oxides, carbon monoxide and uncombusted hydrocarbons from automobile exhaust gases on one hand and as electrode catalysts for fuel cells on the other.[1,2] Aside from these well-established catalysts, it was suggested that the catalytic potential of Ir in this context may not have been fully exploited due to non-chemical factors such as limited availability of the metal and problems with Ir loss.[3] Specifically nitrogen monoxide (NO), the focus of this work, was termed a key air-pollutant by the World Health Organization (WHO) as it affects multiple aspects (water, air and soil) of the environment, while also being hazardous for all forms of life.[4] Although the above named platinum group metals have proven successful for converting NO to N_2, the exact mechanisms underlying the process are not yet fully understood.[5] Therefore, rational design and optimization of existing catalysts - to cut costs and use of scarcely available metals - remains a challenge.

Generally, a metallic catalyst is deposited on oxide supports (such as amorphous silica, alumina or ceria),[6] which further promote the desired reaction. This deposition is operated following three different ways, which each have been given their share of attention. In the first option a metallic alloy is deposited directly onto the oxide leading to issues with adhesion strength, mechanical stability and fracturing of the interfaces.[7] Secondly, single atom catalysis has been investigated, whereby single transition-metal atoms are positioned onto the supporting oxide.[8] However, many challenges remain related to the lifespan activity of these materials due to undesired mobility of the metal atoms over the oxide surface as well as their segregation into the bulk.[9,10] Finally, the aggregation of nanoclusters on oxides after thermal activation has been shown to provide important catalytic performance.[6] It is the latter form that is the focus of this work as the appliance of nanometer-scale metallic particles for the adsorption of CO and NO has been reported successfully in the past.[11]

Most industrial catalysts consist of nanosized particles (clusters) made up of transition-metals, whereby the small size ensures a large active surface area.[12] Furthermore, it

has been suggested that smaller clusters lead to enhanced catalytic activity due to the increasing ratio of atomic sites that are undercoordinated.[13] Obviously, the composition of a given nanocluster is detrimental for the catalytic activity and can lead to three different responses in presence of reactive adsorbates. For the case of NO gas, it was shown that the cluster can remain stable, sinter or dissociate.[14,15] Furthermore, NO itself can react in different ways as it can dissociate (over Rh, Pt and Pd), dimerize (over Cu) upon adsorption or it can simply exhibit molecular adsorption.[16] For effective removal of NO via a DeNOx process, it is the dissociation of NO that is desired, whereby it should be noted that the behavior of the NO adsorbate and the clusters are obviously mutually related.[17]

As numerous temperature-dependent desorption studies have shown that the precise stoichiometry and reaction pathway may depend on the specific local environment of the transition metal, the study of model systems (such as nanoclusters) in a realistic environment are of major importance.[18] The behavior of such nanosized metal clusters on oxide structures has been studied extensively using X-ray absorption spectroscopy (XAS) and Anomalous Wide Angle X-ray Scattering (AWAXS) as they offer information of the atomic arrangement at nanometer scale.[13,19] Indeed, the adsorption of NO to form N_2 and NO_2 on Cu clusters was studied experimentally by Haq et al,[20] while the performance by Ir clusters on alumina has been assessed as well.[21] Furthermore, Pt clusters supported on silica oxides have been reported to be very active for the DeNOx reaction (more active than Ru and Rh) and to be resistant to sintering.[22] However, they have also been shown to deactivate rapidly at low temperatures due to oxygen poisoning.[18] In general, because of the difficult characterization of heterogeneous catalysts both theoretically and experimentally, many unanswered questions remain surrounding the development of more efficient tailored catalysts.[23,24]

From a theoretical point of view, while molecular adsorption of NO has been studied extensively, the focus on dissociative adsorption is rather limited. Using density functional theory, Takagi et al.[25,26] have calculated the activation energies of NO dissociation reactions on several M_{55} clusters (M = Cu, Fe, Co or Ni). These authors

reported that Fe_{55}, Co_{55} and Ni_{55} are reactive toward NO dissociation in agreement with experimental findings, whereby the reactivity followed following order $Fe_{55} > Co_{55} > Ni_{55}$. Deushi et al. calculated the DeNOx reaction pathways on Rh clusters and the Rh (111) surface and predicted that NO dissociation was most favored on small Rh clusters.[27,28] Furthermore, using first principle calculation methods, some of the current authors have investigated the catalytic behavior of seven M_{13} clusters (with M = Pt, Ir, Ru, Rh, Cu, Pd and Ni).[29] Thereby, the adsorption energy for NO and the activation energy for NO dissociation as well as the electronic structure were thoroughly investigated through PBE-D3 functional DFT calculations and compared to previous experimental results. The authors managed to predict the dissociation of NO on the clusters, based on the activation energy and the adsorption energy. The fact that some clusters showed beneficial adsorption energies, but disadvantageous activation energies and vice versa, led them to suggest that 'it is possible to select some bimetallic catalysts with synergistic properties [whereby] a guideline for the choice of the bimetallic system for interesting DeNOx activity would be to add to platinum a second metal such as Rh, Ir of Ru.'[29] Indeed, based on experimental EXAFS analyses, Bazin[19] already stated, back in 2002, that the presence of Rh or other transition metals in small Pt-clusters, may drastically change the behavior of its NO adsorbing capabilities. Similar conclusions were very recently reported by Rodríguez-Kessler et al.[30] in a study on Pt_nCu_n (n = 1,7) clusters, although NO adsorption was not studied specifically. Similarly, bimetallic Au-Pd and Ag-Pd clusters were investigated on their enhanced reactivity and CO adsorption capacities compared to monometallic clusters.[31–33]

As mentioned previously, the behavior of a metal catalyst may be very different as a function of the support material, also depending on their crystalline or amorphous shape, due to the different local environments from one atomic site to another.[34] Much insight has been gained on well-defined crystalline supporting materials as they are easier to study, but amorphous materials are usually cheaper, highly tunable (e.g. porosity) and sometimes their activities may be significantly higher.[35] Indeed, amorphous silica has been shown to be a very efficient support material for metal clusters due to the limited occurrence of strong metal-support interactions, its thermal stability and interesting

mechanical properties.[7] Aside from the amorphous character, also porosity may give strong added benefit to the catalytic activity of nanoclusters as was demonstrated for MOFs.[36,37] However, modelling such amorphous system is hard because their heterogeneity makes identification of active sites very hard. Gierada et al. have recently built an accurate molecular model of a porous silica that allow theoretical predictions in good agreement with experiments, which will be used in this work.[23,38] In addition, a surface variation of the same amorphous silica model has successfully been used to study the Philips catalyst, containing monomeric, dimeric and polymeric chromium on top of amorphous silica.[39,40]

In this work, a Pt_{13} cluster served as reference to assess the influence of doping on the activity for NO dissociation by substituting a Pt atom with either Rh, Ir or Ru. The resulting $Pt_{12}M$ (M = Rh, Ir, Ru) clusters were then used for investigating, at the density functional theory (DFT) level, the adsorption and dissociation behavior of NO. This was done through calculation of the activation energies, adsorption energies, global and local Fermi softness and molecular electrostatic potential of the systems. Furthermore, the clusters were confined into a silica pore to investigate its activity in a more realistic environment, instead of vacuum. Ab initio molecular simulations were performed on this larger system to study its qualitative behavior as a first estimate of the activity of these systems for NO dissociation.

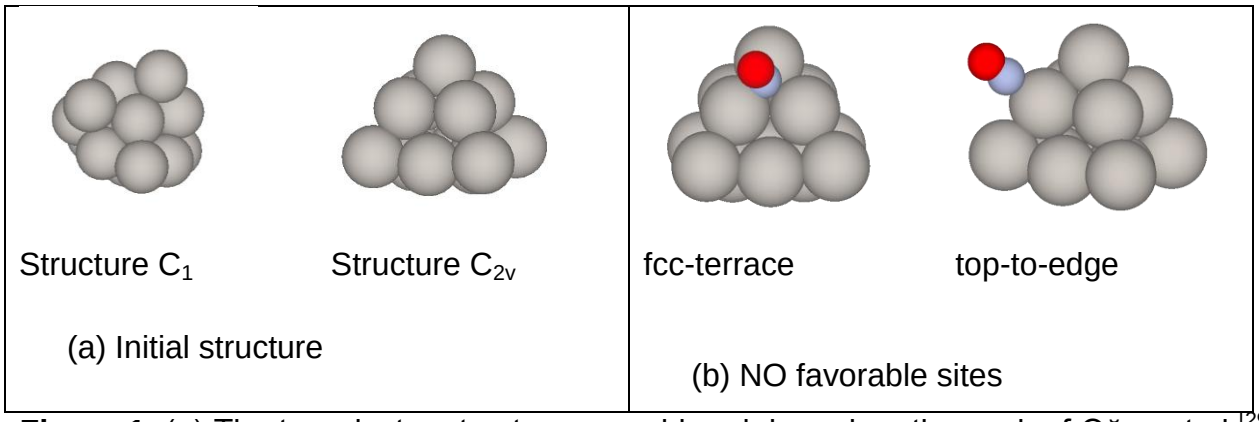

Figure 1. (a) The two cluster structures considered, based on the work of Oğuz et al.[29] and Sun et al.[41] (b) The two adsorption positions considered based on the work of Oğuz et al.[29]

Results and Discussion

Based on the previously mentioned suggestion in the article by Oğuz et al.,[29] three clusters were considered in this work, namely P12Rh, P12Ru and P12Ir, while Pt13 was used as a reference. The stability of such M13 isomers has been investigated in several works and different results have been reported. Sun et al.[41] calculated the minimum energy potential of twelve different structures and reported that a structure with C1 symmetry was the most stable for Pt13. In contrast Oğuz et al. reported the C2v structure to be the most stable one as shown in Figure 1. Therefore, all the considered clusters, Pt13, Pt12Rh, Pt12Ru and Pt12Ir were re-optimized in both configurations to compare their stability. For all clusters, the C2v configuration was found to be the most stable by about 0.35 eV, as shown in Table 1. Furthermore, the substitution of a Pt atom by either Rh, Ru or Ir does not influence the most stable geometry, but it changes the stability of the complex. Indeed, substitution of Pt by Rh, Ru and Ir stabilizes the complex by 1.22 eV, 2.94 eV and 2.15 eV, respectively.

Previous work of Estejab et al.[42] reported DFT calculations on bimetallic PtIr clusters and showed that small molecules prefer to adsorb on the doping atoms, rather than on Pt. On the other hand, Oğuz et al.[29] considered several adsorption geometries for NO on M13 clusters and found the fcc-terrace and top-to-edge sites to be dominant (see Figure 1). Therefore, in this work, one of the top-to-edge positioned Pt atoms was replaced by the chosen substituting atoms so that it would allow adsorption of NO directly on this atom in either the fcc-terrace and top-to-edge sites. Both the fcc-terrace and top-to-edge adsorption sites were then optimized for the Pt12Rh, Pt12Ir and Pt12Ru clusters as can be seen in Figure 2. In all cases, the top-to-edge site was found to be the most favorable by about 0.75 eV and 1.5 eV over the fcc-terrace site, while for P12Ir no stable adsorption was found on the fcc-terrace position. This is not surprising as previous work reported the top-to-edge site to be the most favorable for the Pt13, Rh13, Ru13 and Ir13 clusters.[29] An alternative way to establish the most suitable adsorption site for the NO molecule would consist of determining the local conceptual DFT reactivity descriptors (i.e. Fukui functions or local Fermi softness) for the investigated clusters.

These indices, which describe the response of the system when applying a single perturbation in the external potential and number of electrons, have already been used to differentiate between intramolecular regions that are prone to either nucleophilic or electrophilic attack.[43–46] Due to the hard nature of the NO molecule, it is to be expected that those intramolecular sites of the bimetallic clusters that are defined by low local reactivity indices will be the most suitable for NO adsorption. However, since the fcc-terrace and top-to-edge sites were already shown to be most suitable for adsorption as well as the doped atom, the local reactivity indices were not determined in this work. Overall, the stability order of the different clusters is confirmed upon adsorption of NO on the top-to-edge position with Pt12Ru-NO more stable than Pt12Ir-NO, Pt12Rh-NO and Pt13-NO, in that order. Again, it is seen that the substitution of a Pt atom stabilizes the considered systems.

Next, the transition states for the dissociation of NO on these 4 clusters (Pt13, Pt12Rh, Pt12Ir and Pt12Ru) were determined, whereby it was found that these are similar for all considered clusters. In this state, the O atom of NO tilts towards the top atom and binds to it (see transition states in figure 2). Next, the NO molecule dissociates, whereby the nitrogen atom remains bound to the atom it attacked in the first place and the oxygen atom remains bound to the top atom from the transition state. As such, it seems that the substitution of the top-to-edge Pt atom does not influence the reaction pathway. Although the process does not change qualitatively, the substitutions incur important quantitative differences. Indeed, Table 3 contains the adsorption energies for the four considered clusters where it can be seen that the substitution of a single Pt atom by either one of the three considered metals, stabilizes the adsorption energy substantially. More specifically, the introduction of a Rh atom stabilizes the adsorption energy by 0.34 eV, while the introduction of Ir and Ru stabilizes the adsorption energies by 0.86 eV and 0.87 eV, respectively. In the latter cases, this means a stabilization of about 20 %, which is obviously significant. Furthermore, Oğuz et al.[29] reported adsorption energies of -2.42 eV, -2.41 eV and -2.21 eV for NO on Ir13, Rh13 and Ru13, respectively. As such, the doped cluster in this work display more stable adsorption energies than their monometallic counterparts.

Table 1 : Comparison of total energies calculated with DFT between structure C_1 and C_{2v} for all considered clusters.

Cluster	E_{tot} structure C_1 (eV)	E_{tot} structure C_{2v} (eV)
Pt_{13}	-57.11	-57.46
$Pt_{12}Rh$	-58.29	-58.68
$Pt_{12}Ru$	-59.96	-60.40
$Pt_{12}Ir$	-59.32	-59.61

Comparing these results to their respective surfaces, Zeng et al.[47–49] reported adsorption energies for a single NO molecule between -1.86 eV and -2.43 eV on Rh(111), -1.70 eV and -1.82 eV on Ir(111) and -0.86 eV and -1.77 eV on Pt(111) depending on coverage and adsorption geometry. Ru was not considered, while an adsorption energy of -1.18 eV and -2.34 eV was reported for NO adsorption on Pd(111).

Table 2 : Comparison of total energies for structure C calculated with DFT between the fcc-terrace and top-to-edge adsorption sites for all considered clusters

	E_{tot} fcc-terrace (eV)	E_{tot} top-to-edge (eV)
Pt_{13}-NO	-71.15	-71.93
$Pt_{12}Rh$-NO	-72.59	-73.49
$Pt_{12}Ru$-NO	-74.30	-75.73
$Pt_{12}Ir$-NO	no convergence	-74.92

	Initial State	Transition State	Final State
Pt_{13}	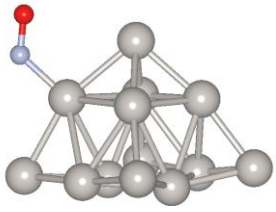	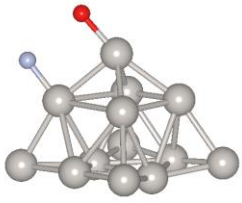	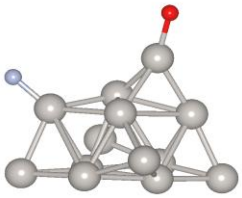

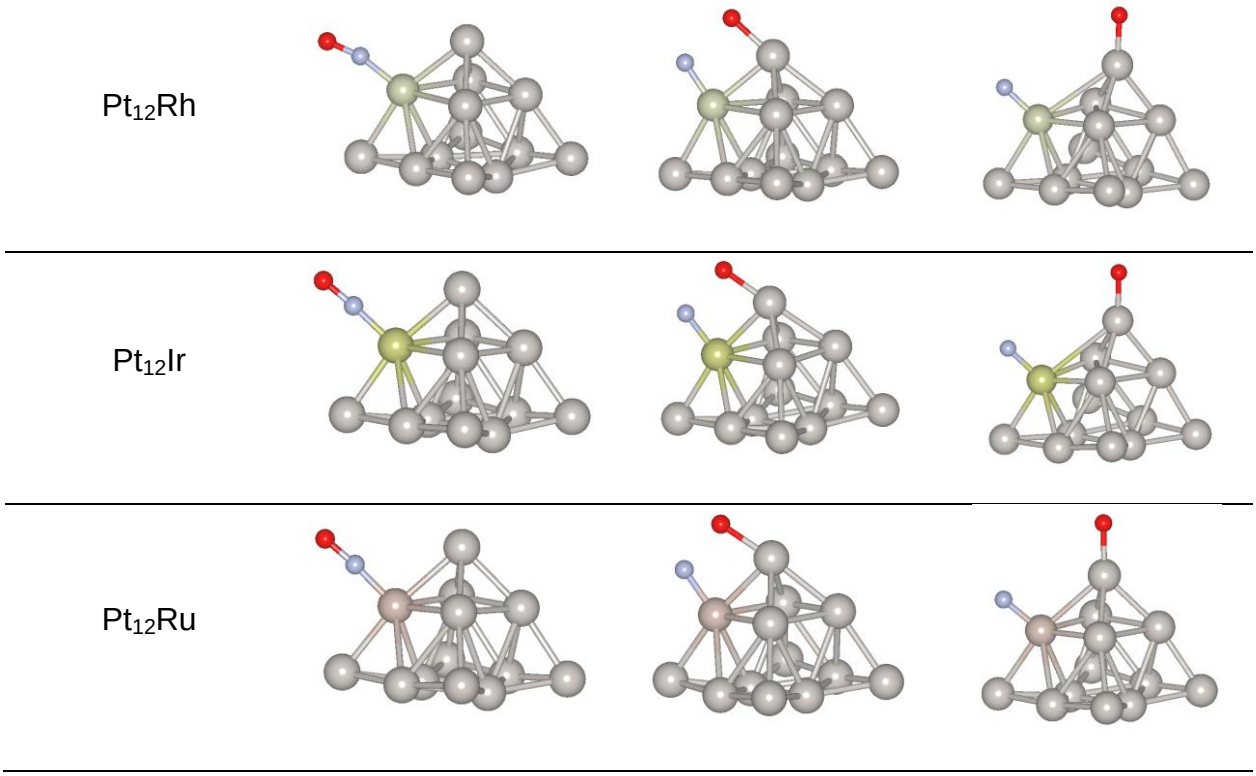

Figure 2. Initial states, transition states and final states for dissociative NO adsorption on all considered clusters.

Furthermore, similar results were reported by Ishikawa et al.[50] and Deushi et al.[51] for NO adsorption on Rh(111). As expected, small clusters show a stronger adsorption energy than their surfaces, while appropriately doping can further enhance the adsorption ability. Importantly, it was shown that adsorption energies can be further influenced by cluster size,[51,52] which is considered outside the scope of this work.

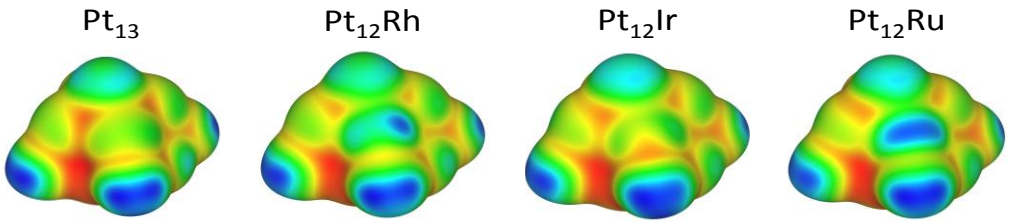

Figure 3. Molecular electrostatic potentials for the plain Pt_{13}, $Pt_{12}Rh$, $Pt_{12}Ir$ and $Pt_{12}Ru$ clusters at an isovalue of 0.005 au.

Another aspect of NO dissociation is the associated activation energy barrier, which should be as low as possible. Again, it is found that the substitution of a single Pt atom in the clusters benefits the dissociation reaction as the activation energy lowers from 2.22 eV for Pt13 to 1.89 eV, 1.70 eV and 1.84 eV for Pt12Rh, Pt12Ir and Pt12Ru, respectively. Importantly, the doping of the Pt13 clusters with a single atom is not enough to lower the activation energy into the range of the monometallic clusters reported by Oguz et al. as they found activation energies of 0.73, 1,16 and 0.63 eV for Ir13, Rh13 and Ru13, respectively. Further in line with their results, the current predictions also follow the maximal hardness principle from which it can be invoked that the harder the transition state is (the more d-electrons that are present, whereby Ru < Rh < Ir), the lower the activation energy will be.

Table 3 : Adsorption energies, activation energies, molecular electrostatic potentials and global softnesses of the considered clusters.

	E_{ads} (eV)	E_{act} (eV)	V_{min} (eV)	$S_{F,rel}$ (eV)
Pt_{13}	-2.17	2.22	-1.65	1.00
$Pt_{12}Rh$	-2.51	1.89	-1.72	0.95
$Pt_{12}Ir$	-3.02	1.70	-1.73	0.45
$Pt_{12}Ru$	-3.03	1.84	-1.77	0.42

Ishikiwa et al. reported an activation energy for NO dissociation between 0.79 eV and 1.76 eV on Rh(111), whereby it should be noted that the lower activation energies required adsorption to a hcp site which is not available in M13 clusters. Deushi et al.[51] reported activation energies between 1.25 eV and 1.38 eV on Rh(111), 0.63 eV and 0.84 eV on Rh55 and 0.68 eV and 0.96 eV on Rh147. Again, the lowest activation energies correspond to hcp sites, which are not available on the small clusters considered here. It should be noted that in general activation energies on small clusters can vary widely (values between 0.23 eV and 2.45 eV have been reported for small Rh6 and Rh7 clusters) depending on cluster geometry and size.[52–55] This is beyond the scope of this work, which focuses on the effect of doping within a given geometry.

Based on the Pearson's hard-soft acid-base (HSAB) principle, it can be assumed that, given the hard chemical character of the considered NO molecule, the largest adsorption energies will be obtained for the hardest metal clusters. As such, the softness (as the inverse of the hardness) of the clusters may be expected to be a good prediction of the adsorption energy (and the activation energy, see above). A first approach to determine the softness of the systems relies on the analysis of Molecular Electrostatics Potentials (MEP). These are generated with respect to a positive charge, which is a typical example of a hard system and indicate electron rich (red) or electron poor (blue) regions. Accordingly, a red region on the MEP, characterized by a negative electrostatic potential, will be very prone to an electrophilic interaction with hard systems as it is an electron-rich environment. Consequently, the more negative the computed electrostatic potential is, the (locally) harder the investigated system.

The MEPs for the different clusters at an isovalue of 0.005 au together with their negative lower limit of the electrostatic potential (Vmin) are schematically represented in Figure 3, while their molecular electrostatic potentials can be found in Table 3. It can be noted that the pure Pt13 cluster is characterized by the least negative electrostatic potential (Vmin = -1.65 eV) and consequently the least pronounced hardness. This is in line with the weaker adsorption of the NO molecule on this cluster as well as the higher activation energy. The substitution of a single Pt atom by an Ir, Rh or Ru seems to positively influence the hardness of the metallic cluster, though the relative differences between the Vmin values of the Pt12M clusters are fairly limited. Indeed, Pt12Ru shows the largest value with an electrostatic potential of -1.77 eV. Nevertheless, it should be remarked that the increasing trend in hardness (Rh < Ir < Ru) perfectly matches with the computed adsorption energies. Therefore, it can be assumed that the hardness of the used metallic cluster plays indeed a crucial role in the adsorption of an NO molecule.

Additionally, global softness of the metallic clusters was calculated, which is a measure of the propensity of the system towards charge transfer and hence inversely related to the hardness. The reactivity index was calculated using a Fermi weighted density of

states approximation as this method has already been shown to give very satisfactory results for catalytic

systems.[8] The introduction of a weight function, defined as the derivative of the Fermi-Dirac distribution function for a given nominal electron temperature (kBT) allows to scale the contributions of successive energy levels to the overall reactivity.

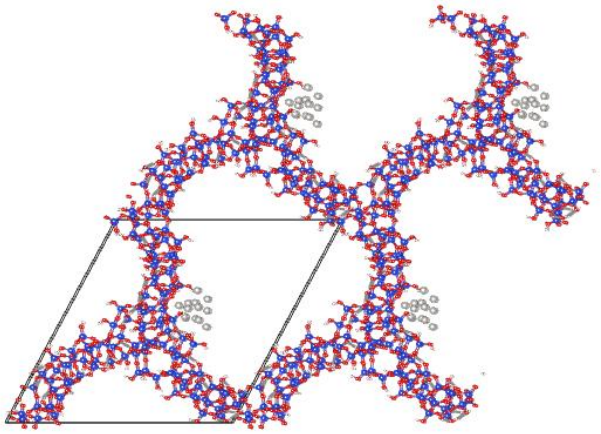

Figure 4: The input structure for the Pt_{13} cluster within the silica pore with the 2 x 2 x 1 supercell. Identical structures were obtained for the remaining clusters. Blue is Si, red is O, white is H and grey is Pt.

according to their relative positions to the Fermi level. In order to determine the most suitable distribution, the Fermi softness (SF) for the four clusters was determined at different temperatures and subsequently correlated to the calculated adsorption energies. For the purpose of simplifying the comparison between the different clusters, it was furthermore decided to employ relative SF values with the softest system being assigned a value of 1.00 eV. The relative Fermi softness for the different kBT options as well as the correlation coefficients can be found in the Supporting Information. With a correlation coefficient of 93%, a nominal electron temperature of 0.15 eV proved to be most suitable for the description of the clusters. The corresponding relative Fermi softness are summarized in Table 3.

It can be noted that the Pt13 complex is described by the largest relative Fermi softness, while the introduction of a single Ru instead of a Pt atom results in the strongest decrease in SF value (0.42 eV). This observation perfectly matches with the trend in

minimal electrostatic potentials. It is also worth noting that the ordering of complexes according to decreasing Fermi softness is identical to that of increasing minimal electrostatic potentials (i.e. increasing hardness). However, unlike the previous discussion of the MEPs, a clear difference in softness between the Pt12Rh and the remaining singly substituted complexes is observed. Indeed, the former complex appears to be much softer as compared to Pt12Ir or Pt12Ru, while hardly any difference is noticeable between the latter two. This finding is in line with the observations in adsorption energy, which indicate that the NO molecule interacts almost as intensively with Pt12Ir or Pt12Ru, but 0.50 eV less strongly with Pt12Rh. Given the strong agreement between the calculated adsorption energies and the molecular electrostatic potentials as well as the relative Fermi softness, it can be concluded with confidence that tuning the hardness of the metallic complex plays a crucial role in the early steps of the NO dissociation.

	Cluster Only	Cluster + NO molecule
Pt_{13}	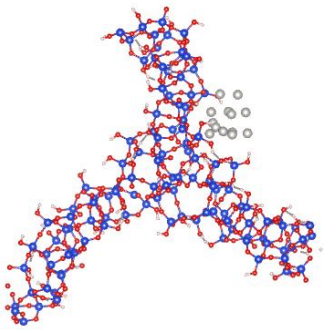	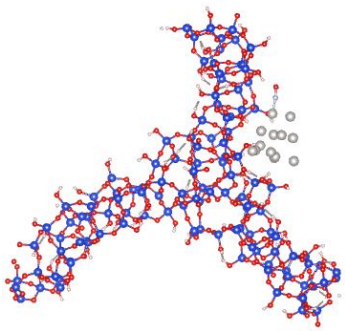

$Pt_{12}Ir$	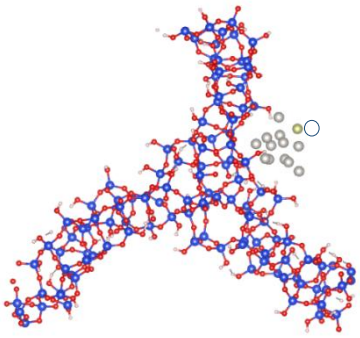	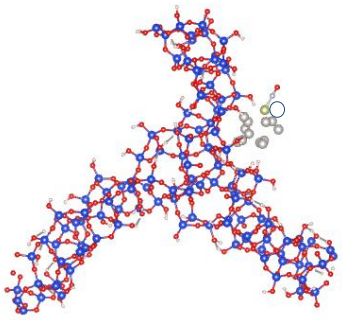
$Pt_{12}Rh$	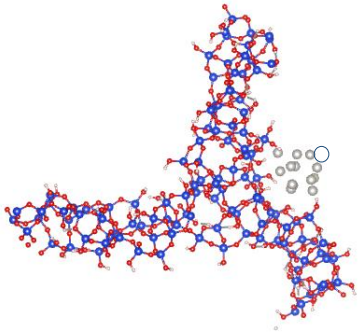	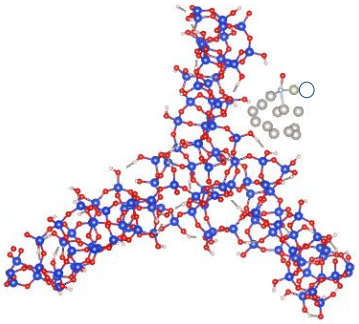
$Pt_{12}Ru$	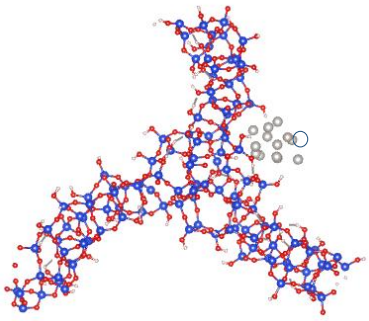	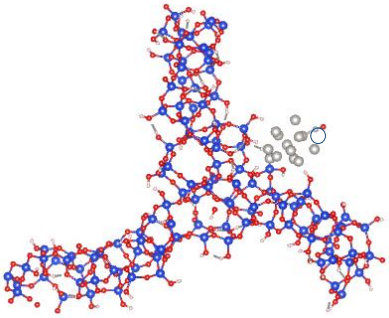

Figure 5. Snapshots of Zthe ab initio simulations after 10 ps for the four considered metal clusters with and without NO molecule adsorbed. Blue is Si, light blue is N, red is O, white is H, grey is Pt, Rh Ru or Ir (the doping atom is circled).

Table 4: Molecular electrostatic potentials and global softnesses of the considered clusters.

	$S_{F,rel}$	$S^-_{F,rel}$
Pt_{13}	0.81	0.92
$Pt_{12}Rh$	1.00	1.00
$Pt_{12}Ir$	0.96	0.92

$Pt_{12}Ru$	0.86	0.81

As mentioned in the introduction, the clusters were then positioned in a pore made up of amorphous silica in order to estimate their behavior in a more realistic environment. The input structure for Pt13 is shown in Figure 4, whereby it can be seen that the optimized Pt13 cluster was positioned in close proximity to the pore surface. Subsequently a series of simulations was performed using ab initio molecular dynamics whereby a Pt atom was replaced by either Ir, Ru or Rh or not replaced at all for reference, similarly to the vacuum calculations. Furthermore, all these simulations were run with and without the presence of an NO molecule located near the (substituted) atom. It should be noted that due to computational constraints, the time scale is limited to 10 ps for computational reasons and only meant as a first estimate of adsorption behavior through calculations of reactivity indices.

In Figure 5, the final snapshots of the different simulations are shown, without NO adsorption on the left and with NO adsorption
on the right. It can be seen that in all cases, the formed clusters lose their original structure and deform somewhat in order to increase contacts with the surface. More specifically, it is seen that the metal atoms position themselves above oxygen atoms preferentially, which is in agreement with previous reported results on Pt deposited on flat Al2O3 surfaces.[56] Apart from this,
the clusters seem to be stable within the cavities and show no signs of fragmentation in all run simulations. On the right side of Figure 5, the final geometries are shown for the metallic clusters with an adsorbed NO molecule. In the case of the Pt12Rh, the adsorbed NO molecule is shared by 2 Pt atom and the Rh atom, while in the other doped clusters as well as the undoped cluster, the NO molecule is always positioned on a single atom. In the case of Rh and Ir, the NO molecule remains located on that atom.

Based on the optimal nominal electron temperature of 0.15 eV for the naked clusters in vacuum, we ultimately computed the local Fermi softness (s_F^-) - describing a potential charge transfer process from the catalytic cluster towards the reagent of interest (NO) - as a tool to predict the strength of the adsorption of a nitrogen oxide molecule.[8] The

choice for this local index - obtained as an integrated product between the Fermi-Dirac weight function and contributions only occurring from the metallic cluster (local density of states) - over an energy range whose upper limit is the Fermi level, is justified by the assumption that nitrogen oxide will mainly interact with the transition metal complex rather than with the amorphous silica zeolite. Overall, an increase in softness relative to the vacuum situation is observed in Table 4, which may suggest that the chosen silica pore is a less suitable choice for clusters aiming at strong interaction with a hard molecule such as NO. However, the increased softness will undeniably lead to more favorable properties for the adsorption of other environmentally toxic, but softer compounds such as for instance carbon monoxide or methane. Nevertheless, the mutual trends between the clusters, with the exception of Pt12Ir, remain fairly well preserved even in the silica pore. As such, the strongest interaction with the NO molecule and thus most favorable adsorption is still to be expected for a cluster consisting of Pt and Ru, as this one is characterized by the lowest relative local Fermi softness index of 0.81 eV. Furthermore, similar to vacuum, the difference in relative softness between the pure Pt13 (0.92 eV) and Pt12Rh (1.00 eV) complexes is rather small (0.08 vs 0.05 eV), although it should be noted that in the silica pore the latter complex is now found to be the softest. The most remarkable difference in softness is however observed for the Pt12Ir complex, where a value identical to that of pure Pt13 is obtained. A potential explanation for this outcome could stem from the fact that Ir and Pt are each others closest neighbors in the periodic system and consequently exhibit rather similar properties. In this context, it might be supposed that in a real chemical environment the response towards a perturbation of a system in which a single platinum atom is replaced by a chemically rather similar Ir atom will not differ too much from the neat Pt13 cluster. According to both our calculations of reactivity indices in vacuum and silica pore, it is suggested that substitution of platinum atoms by ruthenium will positively affect the adsorption of NO molecules.

Conclusions

In this work the potential of bimetallic Pt12M (M = Ru, Rh or Ir) to catalyze NO dissociation, was investigated as compared to a pure Pt13 cluster. In vacuum it was

found that the activation energy for NO dissociation and the adsorption energy of NO on the Pt12M (M = Ru, Rh or Ir) clusters, was lowered by substituting a single Pt atom in the Pt13 suggesting enhanced catalytic capacity of the clusters. Indeed, Pt12Ru, the most favorable cluster, showed an adsorption energy of -3.03 eV and an activation energy of 1.84 eV as compared to -2.17 eV and 2.22 eV, respectively, for Pt13. Following the hard-soft acid-base principle, the calculated adsorption and activation energies correlated well with the softness and the molecular electrostatic potential. Indeed, the harder the cluster, the more favorable it becomes for NO adsorption and subsequent dissociation. Given this good correlation, the global and local softness of the clusters inside a silica pore were calculated to assess the performance of the clusters in a more realistic environment. It was found that the adsorption of the metal clusters in a silica pore softens the system, making them slightly less favorable for NO adsorption, but most likely more efficient for methane and carbon monoxide. On the other hand, the Pt12Ru remained the most suitable cluster for NO dissociation in the silica pore, showing enhanced efficiency compared to Pt13.

Methodology

The naked, spin-polarized clusters were calculated via periodic DFT calculations in the Vienna Ab Initio Simulation Package (VASP) using a plane wave pseudopotential approach.[57] Specifically, the PBE-D3 functional[58] was chosen, as justified by previous work on transition metals,[29,59–61] with a Gaussian smearing of 0.2 eV and a convergence of the electronic self-consistent cycle fixed at 10-6 eV per supercell. Geometries were optimized using the conjugated gradient algorithm until all forces were below 0.01 Å-1. The Projector Augmented-Wavefunction method (PAW) was used to describe the interactions between explicit valence electrons and the ionic cores, allowing an energy-cutoff of 400 eV for the plane-wave basis. To avoid unwanted interactions, the clusters were positioned in a 20 Å x 20 Å x 20 Å unit cell, while the calculations were performed at the Γ-point.

Adsorption energies were calculated by taking the difference in energy between the cluster-NO complex on one hand and the cluster and NO molecule separately, on the other. The transition states corresponding to the bond breaking of adsorbed NO were

determined using the nudge-elastic-band method. Reaction pathways were optimized with a set of eight intermediate geometries. The obtained approximate transition states were refined by minimizing the residual forces below 0.02 eV Å-1 with the quasi-Newton algorithm implemented in VASP. Activation energies were calculated by determining transition states for NO dissociation, whereby 8 (16 in the case of complexes) intermediate geometries were used to optimize the reaction pathways. Vibrational frequencies were calculated within the harmonic approximation to verify all potential energy surface extrema (single imaginary frequency for transition states and positive frequencies for all minima), while the Hessian was computed by finite differences on nuclei forces, followed by a diagonalization procedure to confirm that the resulting eigenvalues correspond the harmonic frequencies.

In order to probe the hard regions of the investigated naked clusters, both the electrostatic potential and charge density were generated by performing a static calculation on the optimized geometry. The molecular electrostatic potential (MEP) was subsequently obtained through plotting of the potential on the charge density, as a three-dimensional isosurface (isovalue = 0.005 au) created with the VESTA software.[62] Starting from the charge density obtained at the Γ-point only, the density of states (DOS) of both the naked cluster in vacuum and in the silica pore was subsequently computed. This DOS was generated over 3000 energy grid points and a (4 x 4 x 4) Γ-centered Monkhorst-Pack k-point grid. These were ultimately used to calculate the global (S_F) and local (s_F) Fermi Softness of these systems as an integrated product, running over an energy range, of a weight function and the total ($g(\varepsilon)$) or local ($g(\varepsilon,\vec{r})$) density of states. The spread of this weight function, which corresponds to the derivative of the Fermi-Dirac distribution function, is subject to a, to be established, nominal electron temperature (k_BT) and reaches a maximum at the Fermi level. As such, it allows to quantify the variable contribution of an energy state to the final reactivity depending on its location with respect to the Fermi level.

$$S_F = \int_{-\infty}^{+\infty} g(\varepsilon)\left(\frac{\partial f(\varepsilon)}{\partial \mu}\right)_{v(\vec{r})} d\varepsilon \qquad (1)$$

$$s_F(\vec{r}) = \int_{\mu \pm \Delta\mu}^{\mu} g(\varepsilon, \vec{r}) \left(\frac{\partial f(\varepsilon)}{\partial \mu} \right)_{v(\vec{r})} d\varepsilon$$

In addition, ab initio molecular dynamics simulations were performed at the DFT-level using the PBE exchange-correlation functional[58] in combination with the D3 Grimme correction[63] (with a cutoff of 16 Å) as implemented in the CP2K/QUICKSTEP package.[64] The DZVP-MOLOPT-GTH basis set was employed and a density cutoff of 350 Ry was used. Periodic boundary conditions were applied in 3 dimensions on a simulation box with dimensions of 36.29 Å x 36.29 Å x 11.60 Å with angles of α = 90°, β = 90 ° and γ = 60°. All simulations were performed in the NVT ensemble using a time step of 0.5 fs for a total simulation time of 10 ps, whereby it should be noted that pre-equilibrated coordinates were used for the pore structure. Convergence was checked via monitoring of scalars such as potential energy and pressure.

Acknowledgements

Computational resources and services were provided by the Shared ICT Services Centre funded by the Vrije Universiteit Brussel, the Flemish Supercomputer Center (VSC) and FWO. The VSC is especially acknowledged for granting a full grant for Tier-1 computation. FDP and FT wish to acknowledge the VUB for support, among other through a Strategic Research Program awarded to their group.

Keywords: Bimetallic Nanoclusters • Transition Metals • DeNOx • DFT • Reactivity indices

References

[1] J. H. Holles, R. J. Davis, J. Phys. Chem. B 2000, 104, 9653–9660.

[2] N. Takagi, K. Ishimura, H. Miura, T. Shishido, R. Fukuda, M. Ehara, S. Sakaki, ACS Omega 2019, 4, 2596–2609.

[3] C. Wögerbauer, M. Maciejewski, A. Baiker, J. Catal. 2002, 205, 157–167.

[4] S. Deutz, D. Bongartz, B. Heuser, A. Kätelhön, L. Schulze Langenhorst, A. Omari, M. Walters, J. Klankermayer, W. Leitner, A. Mitsos, S. Pischinger, A. Bardow, Energy Environ. Sci. 2018, 11, 331–343.

[5] M. J. Piotrowski, P. Piquini, Z. Zeng, J. L. F. Da Silva, J. Phys. Chem. C 2012, 116, 20540–20549.

[6] G. Barcaro, A. Fortunelli, Phys. Chem. Chem. Phys. 2019, 21, 11510–11536.

[7] Q. Fu, T. Wagner, Surf. Sci. Rep. 2007, 62, 431–498.

[8] X. Deraet, J. Turek, M. Alonso, F. Tielens, S. Cottenier, P. W. Ayers, B. M. Weckhuysen, F. De Proft, Chem. – Eur. J. 2021, 27, 6050–6063.

[9] L. Liu, A. Corma, Trends Chem. 2020, 2, 383–400.

[10] Q. Wang, B. Zhu, F. Tielens, D. Tichit, H. Guesmi, Appl. Surf. Sci. 2021, 548, 149217.

[11] F. Tielens, D. Bazin, Comptes Rendus Chim. 2018, 21, 174–181.

[12] J. Kleis, J. Greeley, N. A. Romero, V. A. Morozov, H. Falsig, A. H. Larsen, J. Lu, J. J. Mortensen, M. Dułak, K. S. Thygesen, J. K. Nørskov, K. W. Jacobsen, Catal. Lett. 2011, 141, 1067–1071.

[13] D. Bazin, C. Mottet, G. Tréglia, J. Lynch, Appl. Surf. Sci. 2000, 164, 140–146.

[14] D. Bazin, Macromol. Res. 2006, 14, 230–234.

[15] B. R. Goldsmith, E. D. Sanderson, D. Bean, B. Peters, J. Chem. Phys. 2013, 138, 204105.

[16] W. A. Brown, D. A. King, J. Phys. Chem. B 2000, 104, 2578–2595.

[17] J. M. Bakker, F. Mafuné, Phys. Chem. Chem. Phys. 2022, 24, 7595–7610.

[18] X. Wang, S. M. Sigmon, J. J. Spivey, H. H. Lamb, Catal. Today 2004, 96, 11–20.

[19] D. Bazin, Top. Catal. 2002, 18, 79–84.

[20] S. Haq, A. Carew, R. Raval, J. Catal. 2004, 221, 204–212.

[21] A. Perosa, M. Selva, V. Lucchini, M. Fabris, M. Noè, Int. J. Chem. Kinet. 2011, 43, 154–160.

[22] J. Fu, J. Lym, W. Zheng, K. Alexopoulos, A. V. Mironenko, N. Li, J. A. Boscoboinik, D. Su, R. T. Weber, D. G. Vlachos, Nat. Catal. 2020, 3, 446–453.

[23] F. Tielens, M. Gierada, J. Handzlik, M. Calatayud, Catal. Today 2020, 354, 3–18.

[24] D. Bazin, J. Vekeman, Q. Wang, X. Deraet, F. De Proft, H. Guesmi, F. Tielens, Comptes Rendus Chim. 2022, 25, 1–8.
[25] N. Takagi, M. Ehara, S. Sakaki, ACS Omega 2021, 6, 4888–4898.
[26] N. Takagi, K. Ishimura, R. Fukuda, M. Ehara, S. Sakaki, J. Phys. Chem. A 2019, 123, 7021–7033.
[27] F. Deushi, A. Ishikawa, H. Nakai, J. Phys. Chem. C 2017, 121, 15272–15281.
[28] A. Ishikawa, Y. Tateyama, J. Phys. Chem. C 2018, 122, 17378–17388.
[29] I. C. Oğuz, H. Guesmi, D. Bazin, F. Tielens, J. Phys. Chem. C 2019, 123, 20314–20318.
[30] P. L. Rodríguez-Kessler, A. R. Rodríguez-Domínguez, A. Muñoz-Castro, Phys. Chem. Chem. Phys. 2021, 23, 7233–7239.
[31] J. Creuze, H. Guesmi, C. Mottet, B. Zhu, B. Legrand, Surf. Sci. 2015, 639, 48–53.
[32] J. Wisniewska, H. Guesmi, M. Ziolek, F. Tielens, J. Alloys Compd. 2019, 770, 934–941.
[33] B. Zhu, I. C. Oğuz, H. Guesmi, J. Chem. Phys. 2015, 143, 144309.
[34] B. Peters, S. L. Scott, J. Chem. Phys. 2015, 142, 104708.
[35] B. R. Goldsmith, B. Peters, J. K. Johnson, B. C. Gates, S. L. Scott, ACS Catal. 2017, 7, 7543–7557.
[36] S. O. Odoh, C. J. Cramer, D. G. Truhlar, L. Gagliardi, Chem. Rev. 2015, 115, 6051–6111.
[37] G. Fischer, A. Goursot, B. Coq, G. Delahay, S. Pal, ChemPhysChem 2006, 7, 1795–1801.
[38] M. Gierada, I. Petit, J. Handzlik, F. Tielens, Phys. Chem. Chem. Phys. 2016, 18, 32962–32972.
[39] M. Gierada, P. Michorczyk, F. Tielens, J. Handzlik, J. Catal. 2016, 340, 122–135.
[40] F. Tielens, M. Gierada, J. Handzlik, M. Calatayud, Catal. Today 2020, 354, 3–18.
[41] J. Sun, X. Xie, B. Cao, H. Duan, Comput. Theor. Chem. 2017, 1107, 127–135.
[42] A. Estejab, G. G. Botte, Comput. Theor. Chem. 2016, 1091, 31–40.
[43] R. K. Roy, S. Krishnamurti, P. Geerlings, S. Pal, J. Phys. Chem. A 1998, 102, 3746–3755.
[44] R. K. Roy, F. de Proft, P. Geerlings, J. Phys. Chem. A 1998, 102, 7035–7040.

[45] W. Langenaeker, K. Demel, P. Geerlings, J. Mol. Struct. THEOCHEM 1991, 234, 329–342.
[46] W. Langenaeker, K. Demel, P. Geerlings, J. Mol. Struct. THEOCHEM 1992, 259, 317–330.
[47] Z.-H. Zeng, J. L. F. Da Silva, H.-Q. Deng, W.-X. Li, Phys. Rev. B 2009, 79, 205413.
[48] Z.-H. Zeng, J. L. F. Da Silva, W.-X. Li, Phys. Chem. Chem. Phys. 2010, 12, 2459.
[49] Z.-H. Zeng, J. L. F. Da Silva, W.-X. Li, Phys. Rev. B 2010, 81, 085408.
[50] A. Ishikawa, Y. Tateyama, J. Phys. Chem. C 2018, 122, 17378–17388.
[51] F. Deushi, A. Ishikawa, H. Nakai, J. Phys. Chem. C 2017, 121, 15272–15281.
[52] N. Takagi, K. Ishimura, H. Miura, T. Shishido, R. Fukuda, M. Ehara, S. Sakaki, ACS Omega 2019, 4, 2596–2609.
[53] D. Harding, S. R. Mackenzie, T. R. Walsh, J. Phys. Chem. B 2006, 110, 18272–18277.
[54] H. Xie, M. Ren, Q. Lei, W. Fang, J. Phys. Chem. A 2011, 115, 14203–14208.
[55] N. Takagi, M. Ehara, S. Sakaki, ACS Omega 2021, 6, 4888–4898.
[56] K. Asakura, W.-J. Chun, M. Shirai, K. Tomishige, Y. Iwasawa, J. Phys. Chem. B 1997, 101, 5549–5556.
[57] G. Kresse, J. Furthmüller, Phys. Rev. B 1996, 54, 11169–11186.
[58] J. P. Perdew, K. Burke, M. Ernzerhof, Phys. Rev. Lett. 1996, 77, 3865–3868.
[59] J. Sun, X. Xie, B. Cao, H. Duan, Comput. Theor. Chem. 2017, 1107, 127–135.
[60] C. J. Cramer, D. G. Truhlar, Phys. Chem. Chem. Phys. 2009, 11, 10757.
[61] K. Duanmu, D. G. Truhlar, J. Chem. Theory Comput. 2017, 13, 835–842.
[62] K. Momma, F. Izumi, J. Appl. Crystallogr. 2011, 44, 1272–1276.
[63] S. Grimme, J. Antony, S. Ehrlich, H. Krieg, J. Chem. Phys. 2010, 132, 154104.
[64] T. D. Kühne, M. Iannuzzi, M. Del Ben, V. V. Rybkin, P. Seewald, F. Stein, T. Laino, R. Z. Khaliullin, O. Schütt, F. Schiffmann, D. Golze, J. Wilhelm, S. Chulkov, M. H. Bani-Hashemian, V. Weber, U. Borštnik, M. Taillefumier, A. S. Jakobovits, A. Lazzaro, H. Pabst, T. Müller, R. Schade, M. Guidon, S. Andermatt, N. Holmberg, G. K. Schenter, A. Hehn, A. Bussy, F. Belleflamme, G. Tabacchi, A. Glöß, M. Lass, I. Bethune, C. J.

Mundy, C. Plessl, M. Watkins, J. VandeVondele, M. Krack, J. Hutter, J. Chem. Phys. 2020, 152, 194103.